

ADAPTIVE GAUSSIAN REGULARIZATION CONSTRAINED SPARSE SUBSPACE CLUSTERING FOR IMAGE SEGMENTATION

Sensen Song¹²⁴, Dayong Ren³, Zhenhong Jia^{12*}[†], Fei Shi^{12‡}

¹School of Computer Science and Technology, Xinjiang University, Urumqi, China

²Key Laboratory of Signal Detection and Processing, Xinjiang Uygur Autonomous Region, Urumqi, China

³National Key Laboratory for Novel Software Technology, Nanjing University, Nanjing, China

⁴ College of Mathematics and System Science, Xinjiang University, Urumqi, China

ABSTRACT

Sparse Subspace Clustering (SSC) is integral to image processing, drawing from spectral clustering foundations. However, prevalent methods, relying on an l_1 -norm constraint, fail to capture nuanced inter-region correlations, affecting segmentation efficacy. To remedy this, we introduce an Adaptive Gaussian Regularization Constrained SSC for enhanced image segmentation. This method begins with superpixel preprocessing to enrich local information. Given the Gaussian nature of the SSC's sparse coefficient matrix, a Gaussian probability density function is infused as a regularization term, reinforcing regional image ties and facilitating similarity matrix creation. Using spectral clustering, we then define superpixel clusters leading to the final segmentation. When tested against the BSDS500 and SBD datasets and other leading algorithms, our model showcases marked improvements in natural image segmentation.

Index Terms— SSC, Adaptive, l_1 -norm, Gaussian Regularization, Image Segmentation

1. INTRODUCTION

Subspace clustering, recognized for adept high-dimensional data categorization [1], seeks to assign data points to their pertinent subspace classes. Recently, sparse subspace clustering (SSC), anchored in spectral clustering, has gained traction due to its elegant formulation and robust clustering results. SSC operates by discerning a subspace's representative coefficient matrix, thereby enhancing clustering precision and revealing inherent data structures. This methodology resonates across fields such as machine learning [2], computer vision [3], im-



Fig. 1: Regularization constrained SSC segmentation results based on superpixel image.

age processing [4], pattern recognition [3], and deep learning [5, 6, 7].

SSC hinges on leveraging data sparsity within a determined space for efficient data representation and uncovering intrinsic characteristics. This is achieved by tailoring its data and regularization terms to account for the sparsity and grouping effects of SSC. Sparsity implies data can be represented as a lean combination of a finite dataset, whereas the grouping effect ensures highly correlated data within the same subspace clusters cohesively. In image segmentation, SSC enables the clustering of akin pixels or regions, segmenting the image into distinct regions [8].

However, SSC models with an l_1 -norm [1, 9] offer sparse coefficient matrix representation but stumble in detailing correlations between closely tied data in the same subspace. Conversely, models using nuclear norm [10, 11] or Frobenius norm [12, 13] excel in correlation representation, but lack in matrix sparsity, complicating subspace selection. SSC prioritizes sparse data depiction, while the Low-Rank Representation (LRR) focuses on global data structures. A balance between these two has been a research quest. Some investigations amalgamate low-rank and sparse representations, yet determinations on constraint weights remain elusive. Others engage data-dependent regularization with limited success in reconciling sparsity and grouping, as evidenced in Fig. 1.

In response, we present an adaptive Gaussian regularization constrained SSC for image segmentation, rooted in the hypothesis that SSC's sparse coefficient matrix follows a Gaussian distribution, a conjecture drawn from our matrix observations and Gaussian function properties. The Gaussian function's architecture suggests that with constant variance,

*Corresponding author: Zhenhong Jia

†This work was supported by Tianshan Talent Training Project - Xinjiang Science and Technology Innovation Team Program (2023TSYCTD), National Natural Science Foundation of China (No.62261053), and Research Projects of Basic Research Business Fund for Universities in Xinjiang Autonomous Regions.

‡This work was supported by the Natural Science Foundation of the Xinjiang Uygur Autonomous Region under Grant 2022D01C58.

function values across regions mirror each other with mean value shifts. This property aids in harnessing mean value adjustments to identify data correlations. For image region correlations, two regularization terms with varied mean values constrain the SSC's sparse coefficient matrix.

Spectral clustering typically demands manual clustering number settings, potentially misguiding the clustering. As a remedy, we propose adaptive clustering number determination, leaning on our observations of LRR's adeptness in capturing data's global structure. We utilize its rank value as the clustering number, minimizing the rank of our previously formed sparse coefficient matrix.

Our research's salient contributions include:

- Proposing SSC's sparse coefficient matrix follows a Gaussian distribution, reinforced with a novel Gaussian regularization term. This enriches region correlations, bolstering the similarity matrix's construction and refining segmentation precision.
- Adopting the rank from the LRR-processed sparse coefficient matrix as the clustering count in spectral clustering. This adaptive clustering, content-driven, augments segmentation accuracy.

2. RELATED WORK

Given a dataset $X = [x_1, x_2, \dots, x_N] \in R^{d \times N}$ of N d-dimensional samples $x_i, i = 1, 2, \dots, N$, assume its membership in the union of k linear subspaces $S_{i=1}^k$. The task of subspace clustering is to bifurcate this dataset into distinct sets, each aligned with a specific subspace.

2.1. Superpixel Processing

The relationship between pixel count, information density, and distribution in an image is intrinsically tied to its processing algorithm. To tailor image data for SSC, we employ a superpixel technique. Superpixels [14], essentially compact, semantically meaningful clusters of pixels, embody commonalities in features like texture, color, and luminance. By leveraging intra-pixel similarities, superpixels compactly encapsulate image characteristics, thereby streamlining computational overhead in subsequent stages. This form of preprocessing is pivotal in segmentation paradigms. Specifically, we adopt a superpixel algorithm paralleling the one in the Automatic Fuzzy Clustering Framework for Image Segmentation (AFCF) [15].

The pristine image, of dimensions $321 \times 481 \times 3$, houses 154401 pixels per channel, yielding a similarity matrix sized 154401×154401 . This amounts to data scaling to 10^{10} . Transforming the image via superpixel processing curtails pixel count to a few hundred, compressing the similarity matrix to an order of 10^4 . Consequently, superpixel processing

adeptly curbs data volume while retaining salient local image cues.

2.2. SSC Framework

Within the SSC paradigm, data points are conjectured to be linear combinations of other samples, encapsulated as $X = XZ$, with Z representing the sparse coefficient matrix, indicating inter-sample similarity. The canonical SSC formulation can be expressed as the ensuing optimization challenge, echoing the insights of [16]:

$$\begin{aligned} \min_{Z,E} J(Z) &= \Omega(Z) + \lambda\phi(E) \\ s.t. X &= XZ + E, Z \in R^{N \times N} \end{aligned} \quad (1)$$

Here, $Z \in R^{N \times N}$ demarcates the constraints for matrix Z , $\Omega(Z)$ epitomizes the regularization term, and E typifies perturbations or anomalies. The data fidelity term, $\phi(E)$, quantifies the approximation quality between the represented data XZ and original dataset X .

3. GAUSSIAN REGULARIZED CONSTRAINED SSC MODEL

3.1. Model construction

Traditional l_1 -norm SSC models often fall short in capturing the intricate relationships across various regions in images, thereby undermining their performance in natural image segmentation tasks. To tackle this limitation, we integrate a unique Gaussian regularization term, which prompts the data to be expressed linearly by its most akin counterpart. Specifically, we harness the Gaussian distribution's probability density function of the sparse coefficient matrix, Z , as this regularization term. It's mathematically described as:

$$Z_G(Z | M, \Sigma_n) = \frac{1}{(2\pi)^{N/2} \det^{1/2}(\Sigma_n)} \exp\left(-\frac{1}{2}(Z - \mu_n)^T \Sigma_n^{-1} (Z - \mu_n)\right) \quad (2)$$

Wherein, $Z = z_1, z_2, \dots, z_N$ is defined with M representing the mean matrix, and Σ_n is the corresponding covariance matrix. Both $z_n | n \leq N$ and $\mu_n | n \leq N$ are N -dimensional vectors.

Inspired by the intrinsic Gaussian nature of image features, we hypothesize that the coefficient matrix's relational data should similarly obey varying Gaussian distributions. Such associations can potentially be accentuated by strategically altering the mean values within this matrix. When M represents the average of matrix Z , $Z_G(Z | M, \Sigma_n)$ simplifies to $Z_G^1(Z | M, \Sigma_n)$. The latter effectively boosts the correlation for highly differentiated data, in line with the Gaussian function's inherent attributes. While this is

beneficial for tasks like image clustering, occasional anomalies might emerge. To counteract this, we also introduce a scenario where $M = \mathbf{1}$ (an all-ones matrix), resulting in $Z_G^2(Z | M, \Sigma_n)$, amplifying the data's inherent distinctions. Through this dual formulation, the SSC's correlation representation becomes more dynamic and adjustable.

With these insights, our Gaussian regularized SSC for image segmentation is given by:

$$\begin{aligned} & \min_{Z, A, E} \|Z\|_1 + \lambda_1 \|A \odot Z_G^1\|_F^2 + \lambda_2 \|A \odot Z_G^2\|_F^2 + \delta \|E\|_1 \\ & \text{s.t. } X = XZ + E, A = Z - \text{diag}(Z) \end{aligned} \quad (3)$$

where

$$\begin{aligned} Z_G^1 &= Z_G^1(Z | M, \Sigma_n) \\ Z_G^2 &= Z_G^2(Z | M, \Sigma_n) \end{aligned}$$

$\lambda_1 > 0, \lambda_2 > 0$, and $\delta > 0$ signify the regularizing parameters, and \odot stands for Hadamard product. Solving this model yields the desired matrices, Z and E .

3.2. Optimization

To solve for the sparse coefficient matrix Z of Eq. 3, we employ the Alternating Direction Method of Multipliers (ADMM) [17]. Then its augmented Lagrangian function is given by

$$\begin{aligned} \mathcal{L}(Z, A, E, Y_1, Y_2) &= \|Z\|_1 + \lambda_1 \|A \odot Z_G^1\|_F^2 + \lambda_2 \|A \odot Z_G^2\|_F^2 + \delta \|E\|_1 \\ &+ \langle Y_1, X - XA - E \rangle + \langle Y_2, A - Z + \text{diag}(Z) \rangle \\ &+ \frac{\mu}{2} (\|X - XA - E\|_F^2 + \|A - Z + \text{diag}(Z)\|_F^2) \end{aligned} \quad (4)$$

where $\langle \cdot \rangle$ represents dot product, Y_1 and Y_2 are the matrices of Lagrange multipliers, λ_1 and λ_2 are the control coefficients of Gaussian regularization, δ is the anomaly coefficient, and $\mu > 0$ is a penalty parameter. For each of the five matrices Z, C, E, Y_1 , and Y_2 to be solved in Eq. 4, the cost function is convex if the remaining four matrices are kept fixed. We update each of them alternately while keeping the others fixed.

(1) *Update for Z :* We update Z by solving the following problem,

$$\begin{aligned} Z^{t+1} &= \arg \min_Z \|Z\|_1 + \langle Y_2^t, A^t - Z + \text{diag}(Z) \rangle \\ &+ \frac{\mu^t}{2} \|A^t - Z + \text{diag}(Z)\|_F^2 \\ &= \arg \min_Z \|Z\|_1 + \|Z - \text{diag}(Z) - A^t - \frac{Y_2^t}{\mu^t}\|_F^2 \\ &= S_{\frac{1}{\mu^t}}(A^t + \frac{Y_2^t}{\mu^t}) \end{aligned} \quad (5)$$

where $S_\tau(\cdot)$ is the shrinkage thresholding operator.

(2) *Update for A :*

$$\begin{aligned} A^{t+1} &= \arg \min_A \lambda_1 \|A \odot Z_G^1\|_F^2 + \lambda_2 \|A \odot Z_G^2\|_F^2 \\ &+ \langle Y_1^t, X - XA - E^t \rangle \\ &+ \langle Y_2^t, A - Z^{t+1} + \text{diag}(Z^{t+1}) \rangle \\ &+ \frac{\mu^t}{2} \|X - XA - E^t\|_F^2 \\ &+ \frac{\mu^t}{2} \|A - Z^{t+1} + \text{diag}(Z^{t+1})\|_F^2 \\ &= \arg \min_A \frac{\lambda_1}{\mu^t} \|A \odot Z_G^1\|_F^2 \\ &+ \frac{\lambda_2}{\mu^t} \|A \odot Z_G^2\|_F^2 \\ &+ \|Z^{t+1} - \text{diag}(Z^{t+1}) - A^t - \frac{Y_2^t}{\mu^t}\|_F^2 \\ &+ \|X - XA - E^t + \frac{Y_1^t}{\mu^t}\|_F^2 \end{aligned} \quad (6)$$

It can be found that the Eq. 6 is a convex optimization problem, and we can obtain the optimal solution for A by deriving Eq. 6.

$$\begin{aligned} A^{t+1} &= (X^T X + I - \frac{\lambda_1}{\mu^t} (Z_G^1)^2 - \frac{\lambda_2}{\mu^t} (Z_G^2)^2)^{-1} \\ &\cdot (X^T (X - E^t + \frac{Y_1^t}{\mu^t}) + Z^{t+1} - \text{diag}(Z^{t+1}) - \frac{Y_2^t}{\mu^t}) \end{aligned} \quad (7)$$

(3) *Update for E :*

$$\begin{aligned} E^{t+1} &= \arg \min_E \delta \|E\|_1 + \langle Y_1^t, X - XA^{t+1} - E \rangle \\ &+ \frac{\mu}{2} \|X - XA^{t+1} - E\|_F^2 \\ &= \arg \min_E \frac{\delta}{\mu^t} \|E\|_1 + \|X - XA^{t+1} - E + \frac{Y_1^t}{\mu^t}\|_F^2 \\ &= S_{\frac{\delta}{\mu^t}} \left(X - XA^{t+1} + \frac{Y_1^t}{\mu^t} \right) \end{aligned} \quad (8)$$

(3) *Update for Y_1 and Y_2 :* The Lagrange multiplier matrices Y_1 and Y_2 are updated based on a gradient descent method:

$$Y_1^{t+1} = Y_1^t + \mu^t (X - XA^{t+1} - E^{t+1}) \quad (9)$$

$$Y_2^{t+1} = Y_2^t + \mu^t (A - Z^{t+1} + \text{diag}(Z^{t+1})) \quad (10)$$

For the sake of lucidity, we present Algorithm 1, which encapsulates the ADMM (Alternating Direction Method of Multipliers) approach for resolving the optimization problem outlined in Eq. (4).

We can address the optimization problem presented in Eq. 3 using Algorithm 1, which furnishes us with the sparse coefficient matrix Z . Subsequently, we implement spectral

Algorithm 1: ADMM for Solving Problem (3)

Data: $X \in R^{d \times N}$, λ_1 , λ_2 , and δ
Result: $Z \in R^{N \times N}$

- 1 $Z^0 = A^0 = E^0 = V^0 = Y^0 \leftarrow 0 \in R^{N \times N}$, $t \leftarrow 0$, $\lambda_1 = 5$, $\lambda_2 = 2$, $\delta = 0.8$, $\mu^0 = 0.1$, $\rho = 2$, $\epsilon = 10^{-8}$;
- 2 **while** $\|X - XA^{t+1} - E^{t+1}\|_\infty < \epsilon$ **do**
- 3 Update Z^{t+1} , A^{t+1} , and E^{t+1} using Eq. 5, Eq. 7, and Eq. 8;
- 4 Update Y_1^{t+1} and Y_2^{t+1} using Eq. 9 and Eq. 10;
- 5 $\mu^{t+1} \leftarrow \rho\mu^t$;
- 6 **end**

clustering on the Laplacian matrix, derived from the similarity matrix W , where $W = |Z| + |Z|^T$. This leads us to the outcome of image clustering segmentation. Furthermore, to facilitate automated image segmentation, we leverage the rank of the sparse coefficient matrix Z —obtained through LRR—as the cluster count for the spectral clustering algorithm. This approach is predicated on the proficiency of LRR in capturing the global structure inherent in the image.

4. EXPERIMENTS

4.1. Evaluation of Gaussian Regularization

In Eq. 3, we enhance the l_1 -norm SSC with two Gaussian regularization terms characterized by distinct means, modulated by parameters λ_1 and λ_2 . A comprehensive experimental series was executed to delineate the efficacy of these regularization terms and the sensitive dynamics influenced by the variable coefficients in image clustering.

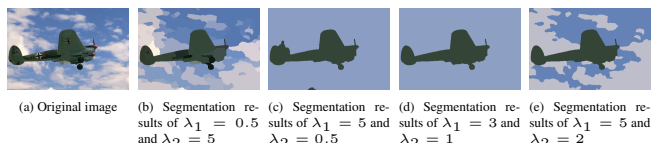


Fig. 2: The effects of Gaussian regularization control coefficients λ_1 and λ_2 on the image segmentation results.

Fig. 2 delineates the segmentation ramifications of different λ_1 and λ_2 configurations: At $\lambda_1 = 0.5$ and $\lambda_2 = 5$, Fig. 2(b) evidences a palpable over-segmentation, with numerous superpixels remaining disparate. Contrarily, $\lambda_1 = 5$ and $\lambda_2 = 0.5$ induce a substantial amalgamation of highly differentiated superpixels, as seen in Fig. 2(c), fostering suboptimal segmentation. A near-ideal concordance with the ground truth is achieved in Fig. 2(d) with parameters $\lambda_1 = 3$ and $\lambda_2 = 1$. Fig. 2(e) optimally leverages empirically determined parameter values to attain superior segmentation outcomes.

Our experiments substantiate that a higher emphasis on

Z_G^2 attenuates the constraining influence of the regularization term, a phenomenon grounded in its facilitative role in heightening differentiation amongst image regions. On the other hand, a pronounced Z_G^1 influence fosters enhanced correlation between distinct regions, albeit risking over-aggregation with excessive weighting as manifested in Fig. 2(c). Optimal metric performance, evidenced through rigorous evaluations, is observed with coefficients at $\lambda_1 = 5$ and $\lambda_2 = 2$.

Furthermore, Table 1 showcases the proposed algorithm exhibiting improved fit and enhanced correlation representation in l_1 -norm SSC when compared to the traditional SSC model, validating the robust augmentative role of the Gaussian regularization term in enhancing image segmentation performance.

Table 1: Performance comparison of different algorithms on the BSDS500 and SBD datasets. The best values are highlighted.

Methods	PRI \uparrow		VoI \downarrow		GCE \downarrow		BDE \downarrow	
	BSDS500	SBD	BSDS500	SBD	BSDS500	SBD	BSDS500	SBD
SSC	0.68	0.70	2.33	2.01	0.18	0.16	19.98	18.17
SFFCM	0.72	0.74	2.31	1.93	0.26	0.20	14.35	11.57
AFCF	0.74	0.79	2.05	1.85	0.22	0.17	12.95	11.08
AF-graph	0.79	0.78	2.01	1.78	0.21	0.19	13.01	10.91
OURS	0.79	0.81	2.20	1.78	0.17	0.18	12.88	10.56

4.2. Experiments on BSDS500 and SBD Datasets

To validate the superiority of our proposed method, we benchmarked on the BSDS500 [18] and SBD [19] datasets. Evaluation was rigorous, adopting four prevalent metrics [20]: PRI, VoI, GCE, and BDE. We juxtaposed our results with four state-of-the-art techniques: SSC, AFCF [15], AF-graph [20], and SFFCM [21].

Table 1 presents the performance comparison between the proposed algorithm and the comparative algorithms across four evaluation metrics. On the BSDS500 dataset, our proposed algorithm showcases excellence in PRI, GCE, and BDE metrics, but trails behind the comparative algorithms AF-graph and AFCF in terms of the VoI metric. Moreover, on the SBD dataset, our method exhibits superior performance in PRI, VoI, and BDE metrics. However, it does not match the performance of the comparative algorithms SSC and AFCF regarding the GCE metric. In conclusion, our proposed method outperforms the comparative methodologies and yields high-quality segmentation results in unsupervised image clustering.

5. CONCLUSION

This paper introduces an adaptive Gaussian regularization constrained sparse subspace clustering technique tailored for

image segmentation, addressing the l_1 -norm SSC's limitations. Harnessing Linear Robust Representation, we encapsulate global structural information, guiding adaptive clustering through the rank of its coefficient matrix. Experimental validations underscore the algorithm's superiority in revealing intricate correlations within diverse image regions, pushing the frontier of image segmentation performance.

6. REFERENCES

- [1] Ehsan Elhamifar and René Vidal, “Sparse subspace clustering: Algorithm, theory, and applications,” *IEEE Transactions on Pattern Analysis and Machine Intelligence*, vol. 35, no. 11, pp. 2765–2781, 2013.
- [2] M. I. Jordan and T. M. Mitchell, “Machine learning: Trends, perspectives, and prospects,” *Science*, vol. 349, no. 6245, pp. 255–260, 2015.
- [3] John Wright, Yi Ma, Julien Mairal, Guillermo Sapiro, Thomas S. Huang, and Shuicheng Yan, “Sparse representation for computer vision and pattern recognition,” *Proceedings of the IEEE*, vol. 98, no. 6, pp. 1031–1044, 2010.
- [4] G. P. Obi Reddy, *Digital Image Processing: Principles and Applications*, pp. 101–126, Springer International Publishing, Cham, 2018.
- [5] Zhihao Peng, Yuheng Jia, Hui Liu, Junhui Hou, and Qingfu Zhang, “Maximum entropy subspace clustering network,” *IEEE Transactions on Circuits and Systems for Video Technology*, vol. 32, no. 4, pp. 2199–2210, 2021.
- [6] Zhihao Peng, Hui Liu, Yuheng Jia, and Junhui Hou, “Adaptive attribute and structure subspace clustering network,” *IEEE Transactions on Image Processing*, vol. 31, pp. 3430–3439, 2022.
- [7] Ling Zhao, Yunpeng Ma, Shanxiong Chen, and Jun Zhou, “Deep double self-expressive subspace clustering,” in *ICASSP 2023-2023 IEEE International Conference on Acoustics, Speech and Signal Processing (ICASSP)*. IEEE, 2023, pp. 1–5.
- [8] Wencheng Zhu, Jiwen Lu, and Jie Zhou, “Nonlinear subspace clustering for image clustering,” *Pattern Recognition Letters*, vol. 107, pp. 131–136, 2018.
- [9] Yingya Zhang, Zhenan Sun, Ran He, and Tieniu Tan, “Robust subspace clustering via half-quadratic minimization,” in *2013 IEEE International Conference on Computer Vision*, 2013, pp. 3096–3103.
- [10] Jinhui Chen and Jian Yang, “Robust subspace segmentation via low-rank representation,” *IEEE Transactions on Cybernetics*, vol. 44, no. 8, pp. 1432–1445, 2014.
- [11] Ming Yin, Junbin Gao, and Zhouchen Lin, “Laplacian regularized low-rank representation and its applications,” *IEEE Transactions on Pattern Analysis and Machine Intelligence*, vol. 38, no. 3, pp. 504–517, 2016.
- [12] Xi Peng, Canyi Lu, Zhang Yi, and Huajin Tang, “Connections between nuclear-norm and frobenius-norm-based representations,” *IEEE Transactions on Neural Networks and Learning Systems*, vol. 29, no. 1, pp. 218–224, 2018.
- [13] Song Yu and Wu Yiquan, “Subspace clustering based on latent low rank representation with frobenius norm minimization,” *Neurocomputing*, vol. 275, pp. 2479–2489, 2018.
- [14] Radhakrishna Achanta, Appu Shaji, Kevin Smith, Aurelien Lucchi, Pascal Fua, and Sabine Süsstrunk, “Slic superpixels compared to state-of-the-art superpixel methods,” *IEEE Transactions on Pattern Analysis and Machine Intelligence*, vol. 34, no. 11, pp. 2274–2282, 2012.
- [15] Tao Lei, Peng Liu, Xiaohong Jia, Xuande Zhang, Hongying Meng, and Asoke K. Nandi, “Automatic fuzzy clustering framework for image segmentation,” *IEEE Transactions on Fuzzy Systems*, vol. 28, no. 9, pp. 2078–2092, 2020.
- [16] Han Hu, Zhouchen Lin, Jianjiang Feng, and Jie Zhou, “Smooth representation clustering,” in *2014 IEEE Conference on Computer Vision and Pattern Recognition*, 2014, pp. 3834–3841.
- [17] Stephen Boyd, Neal Parikh, Eric Chu, Borja Peleato, and Jonathan Eckstein, *Distributed Optimization and Statistical Learning via the Alternating Direction Method of Multipliers*, 2011.
- [18] Pablo Arbeláez, Michael Maire, Charless Fowlkes, and Jitendra Malik, “Contour detection and hierarchical image segmentation,” *IEEE Transactions on Pattern Analysis and Machine Intelligence*, vol. 33, no. 5, pp. 898–916, 2011.
- [19] Stephen Gould, Richard Fulton, and Daphne Koller, “Decomposing a scene into geometric and semantically consistent regions,” in *2009 IEEE 12th International Conference on Computer Vision*. IEEE, 2009, pp. 1–8.
- [20] Yang Zhang, Moyun Liu, Jingwu He, Fei Pan, and Yanwen Guo, “Affinity fusion graph-based framework for natural image segmentation,” *IEEE Transactions on Multimedia*, vol. 24, pp. 440–450, 2022.
- [21] Tao Lei, Xiaohong Jia, Yanning Zhang, Shigang Liu, Hongying Meng, and Asoke K. Nandi, “Superpixel-based fast fuzzy c-means clustering for color image segmentation,” *IEEE Transactions on Fuzzy Systems*, vol. 27, no. 9, pp. 1753–1766, 2019.